Journal of Alloys and Compounds 495 (2010) 446–449

Contents lists available at ScienceDirect

Journal of Alloys and Compounds

journal homepage: www.elsevier.com/locate/jallcom

Carbon nanotubes and nanofibers synthesized by CVD on nickel coatings deposited with a vacuum arc

M. Escobar[a,b], L. Giuliani[c], R.J. Candal[d], D.G. Lamas[e], A. Caso[a], G. Rubiolo[a,f], D. Grondona[c], S. Goyanes[a], A. Márquez[c,*]

[a] LP&MC, Dep. de Fisica-FCEyN-UBA, Cdad. Universitaria Pab.1, (1428), Buenos Aires, Argentina
[b] DQIAQF-FCEyN-UBA, Cdad. Universitaria Pab.1, (1428), Buenos Aires, Argentina
[c] INFIP, CONICET, Dep. de Física, FCEyN-UBA, Cdad. Univ. Pab.1, (1428), Buenos Aires, Argentina
[d] INQUIMAE-FCEyN-UBA, Cdad. Universitaria Pab.2, (1428), Buenos Aires, Argentina
[e] CINSO, CITEFA, CONICET, J.B. de La Salle 4397, (1603) V.Martelli, Buenos Aires, Argentina
[f] UAM-CNEA, Av. Gral Paz 1499, (1650) San Martín, Buenos Aires, Argentina

ARTICLE INFO

Article history:
Received 25 July 2008
Received in revised form 29 October 2009
Accepted 4 November 2009
Available online 11 December 2009

Keywords:
Nanostructured materials
Thin films

ABSTRACT

Nanotubes and nanofibers were grown on Ni coatings deposited by plasma generated with a pulsed vacuum arc on silicon wafers using three different bias conditions: at floating potential (approximately +30 V respect to the grounded cathode); at ground potential; and at −60 V. An atomic force microscopy study showed that the Ni film morphology was affected by the bias condition of the substrate. The morphology of carbonaceous species depended on Ni-films characteristics. FE-SEM and TEM analyses have shown that nanofibers growth was favoured on Ni coatings deposited at −60 V whereas nanotubes grew mainly on Ni coatings obtained at floating and ground potentials. Hence, this new method to produce the precursor can be optimized to obtain nanotubes or nanofibers varying the substrate bias for the Ni deposition.

1. Introduction

Carbon nanostructures (CNS) have attracted much interest since their discovery and many studies have been carried out due to their large potential applications. In particular, CNS filaments are good candidates for field emission applications [1]. Chemical Vapor Deposition (CVD) is a promissory method to synthesize CNS, due to its simple configuration and flexibility in the adjustment of the parameters which control the CNS growth [2–4].

Nanoparticles of metal transition (Fe, Ni, Co) act as nucleation centers for the growth of CNS and catalyze the decomposition of the carbon source [5]. The properties of a nanostructured catalyst influences on the CVD synthesis of CNS. Several methods have been proposed to prepare systems containing metal nanoparticles supported on different substrates [6,7], in particular on conductive smooth surface substrates, as it is required for the application of the CNS to field emission. In this paper, the method employed to deposite Ni films was a pulsed vacuum arc discharge. Its main advantages, compared to the standard sputtering process, are the highly ionized state of the evaporated material, the absence of gases to sustain the discharge (that not only eliminates the rare gas contamination from the film, but also reduces the possible contamination from the impurities present in the sputtering gas or eventually from leaks in the injection line), and the relatively high energy (about 30 eV) of atoms reaching the substrate surface. In these devices, a high current (>100 A) runs between the electrodes generating the emission of a metallic plasma jet from the cathode. When a substrate is located intercepting the plasma jet, a metallic coating is obtained. If a non-insulating substrate is employed, applying a negative bias to the sample, the ion impinging energy on the surface can be increased. As the particle energy has a direct influence on the film microstructure, the coating characteristics can be modified changing this parameter.

The aim of this work has been to analyze the influence of the nanostructure Ni film properties on CNS-grown characteristics carrying out a systematic study on the nickel deposition conditions.

2. Experimental

2.1. Nanostructured Ni-film

The nickel films were deposited onto silicon substrates with a vacuum arc discharge [8]. The arc was pulsed for ∼35 ms, with an arc peak current of (450 ± 20) A and an inter-electrode voltage of (45 ± 5) V. The arc was produced by discharging an electrolytic capacitor bank with $C = 0.075$ F, connected to a series inductor–resistor ($L = 2$ mH, $R = 0.33\ \Omega$), which critically damped the discharge. A grounded Ni cathode was located in front of an annular anode. At the end of the anode, the entrance of a magnetic duct was placed with a magnetic field strength at the axis of 290 G. The

---

[*] Corresponding author. Tel.: +54 11 4576 3371; fax: +54 11 4787 2712.
E-mail address: amarquez@df.uba.ar (A. Márquez).

0925-8388/$ – see front matter © 2009 Elsevier B.V. All rights reserved.
doi:10.1016/j.jallcom.2009.11.162

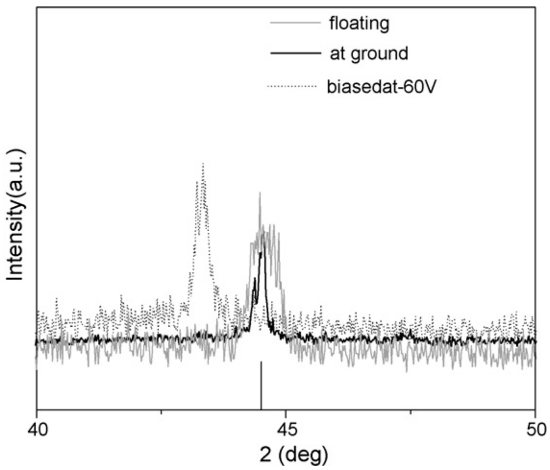

Fig. 1. XRD patterns of Ni films grew at different potentials.

silicon substrate was placed at 10 cm from the cathode tip into the magnetic duct. The silicon substrate was one-side polish, B-doped, p-type and (1 0 0)-oriented. The Ni films were obtained with two discharges performed on the polish side of the silicon substrate. Ni coatings were deposited at three different bias conditions, at floating potential; at ground potential; and at −60 V respect to the ground. These three bias conditions produce an effective acceleration voltage for the ions to the substrate of 0 V, −30 V, −90 V taking into account that in this device the plasma potential respect to ground is approximately 30 V. Three samples were made, for each bias condition, in order to check repetitivity. The film thickness was estimated from the measurement of the average charge collected by the sample.

The crystalline structure of the films was identified by X-ray diffraction (XRD) using a Philips PW 3710 diffractometer with a Cu Kα source. It was operated with glancing angle geometry by using a Philips thin film attachment, with an angle of incidence of 1°. The Ni film morphology was studied by tapping mode atomic force microscopy (AFM) with a Nanoscope III Digital-VEECO.

2.2. CNS growth

CNS were grown by CVD on silicon substrates coated with Ni deposited as described above. The substrates were placed in a quartz boat and introduced into a chamber of a tube furnace. The chamber was purged by pumping with a mechanical vacuum pump, followed by the injection of a 9% hydrogen/nitrogen mixture, with a flow of 100 sccm, at 180 torr. The temperature was raised from room temperature to 700 °C, with a ramp of 15 °C/s. This treatment allowed to reduce the nickel oxide that could be generated as consequence of the exposure of the film to air. After the temperature reach 700 °C, acetylene (10 sccm) was introduced as carbon source keeping the above condition. The growth time was 20 min. After the growth of CNS, the furnace was cooled to the room temperature in a nitrogen flow.

Transmission electron microscopy (TEM-EM Philips 301) and Field Emission Scanning Electron Microscopy (FEG-SEM Zeiss LEO 982 GEMINI) were employed to study the different morphologies. For the TEM studies the samples of CNS were detached from the catalyst by ultrasonic dispersal in ethanol.

3. Results and discussion

The Ni films covered an area of 0.8 cm^2. The average charge impinging on the surface (Q) was 2.7×10^{-3} C. Taking into account the Q value, an average charge state number of the ions of 1.8, the coated area and the Ni density, the thickness of the layer deposited in each discharge was estimated in 1.2 nm. When the scotch test was performed detached of material from the Ni films was not detected indicating that the films presented a good adhesion to the substrate. XRD results allowed to determine that all films grew crystallized. The diffractograms of the films deposited at different bias voltages are depicted in Fig. 1. The films grew at floating and ground potential presented a Bragg peak corresponding to Ni (1 1 1). In the case of the samples biased at −60 V, it was registered a peak at $2\theta = 43.2°$ that agrees with the 2θ position of a NiO Bragg peak. Then, Ni films were obtained with the lower absolute values of bias voltages while at −60 V a nickel compound was found. The formation of this nickel compound could be promoted by the heating of the substrate surface due to the collection of a fraction of the main current discharge on the sample. This phenomenon could be induced by the high negative potential.

Fig. 2 displays AFM images of the surface of Ni films, for the different bias conditions, taken before the samples were placed in the CNT reactor. The film surfaces were dense, composed of columnar grains with a distance between the column top of the same size as the column width and without the presence of voids. The films deposited at floating potential (Fig. 2a) showed the growth of some isolated columns of approximately 10 nm in height on a smooth surface. From the AFM registers the estimated grain size was 1 nm in height and ~10 nm width.

The sample coated at ground potential (Fig. 2b) exhibited the smoothest surface with grains smaller than 10 nm in width and 1 nm in height. Whereas the films deposited at −60 V (Fig. 2c) presented grains between 20 and 50 nm in width and 10 nm in height. These results indicated that the morphology of the films was strongly affected by the bias voltage applied on the silicon substrate during the deposition procedure.

Fig. 3 shows SEM micrograph of CNS layers synthesized by CVD on Ni-films deposited at the three bias conditions. The obtained CNS layers on Ni-films deposited at floating (Fig. 3a$_1$) and at ground potential (Fig. 3b$_1$) were homogeneous layers, while those grew on Ni-films deposited at −60 V (Fig. 3c$_1$) were inhomogeneous layers with marked cracks. Fig. 3a$_2$, 3b$_2$ and 3c$_2$ correspond to the same samples but with higher magnification.

Fig. 4 shows TEM micrograph of CNS. CNS grown on the Ni-films deposited at floating potential (Fig. 4a) and at ground (Fig. 4b) were typically multiple wall carbon nanotubes (MWCNT), with similar internal diameters (4–7 nm) and external diameters in the range 17–50 nm and 17–30 nm, respectively. In the first case, the wider external diameter was consequence of the great amount of amorphous carbon deposited on the external wall of the MWCNT (see the light gray area surrounded the crystalline internal walls). The CNS grown on samples obtained at −60 V (Fig. 4c) were mostly helical carbon nanofibers (HCNF) and few MWCNT characterized by a wide internal channel, about 40 nm (Fig. 4d). In Fig. 5 FE-SEM image with a detail of the HCNF is shown, it can be noticed that the HCNF were coated by carbon nanoparticles [9].

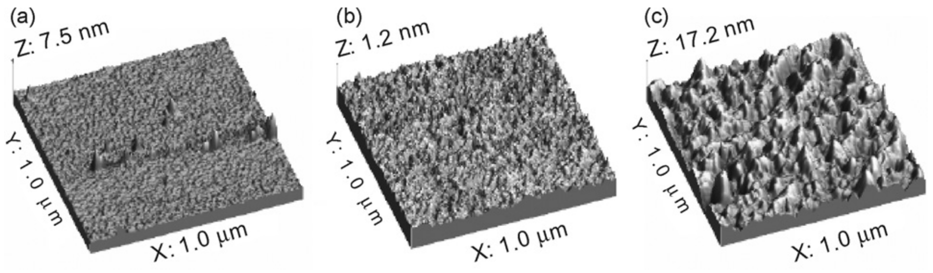

Fig. 2. AFM images of Ni-films obtained at (a) floating potential, (b) ground potential, and (c) −60 V.

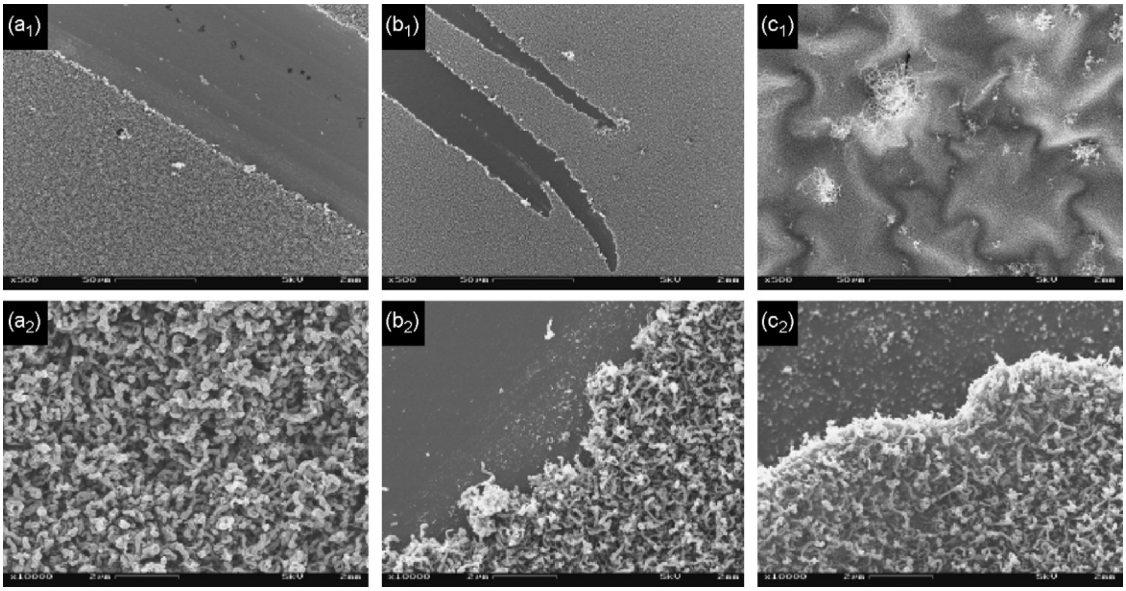

Fig. 3. FE-SEM images of carbon nanostructures obtained: (a) floating potential, (b) ground potential, and (c) −60 V. Subscript '1' corresponds to a 500× magnification and subscript '2' corresponds to a 10,000× magnification.

Considering the Ni-film morphologies (Fig. 2), the characteristic of CNS grown on each one (Fig. 4) lead to the idea that the amount of active nucleation centers for the growth of the MWCNT, by unit area, was bigger as smoother the Ni film surface was. The differences in the morphology of the Ni films could be accentuated during the CNS growth process. As a result of the high temperature of the process (700 °C), the initial columnar grain size is modified due to the migration of nickel atoms (or cluster) on the surface, leading to the formation of domes with different sizes. Depending on the size of the domes, which act as nucleation centers, different CNS are grown on the substrates. On the Ni films with the initial lowest roughness, nanotubes with the lowest amount of amorphous carbon were obtained. The domes on Ni-films deposited at −60 V should evolve to a larger diameter promoting the growth of the nanofibers. The amount of amorphous carbon observed on the CNS walls could be associated to the number of nucleation active centers: the small number of nucleation active centers lead to the excess of carbon which precipitated as amorphous carbon on the walls of CNS, in agreement with other works [10,11]. The nanofibers growth could also be favoured by the presence of a Ni compound.

From TEM micrograph (see Fig. 4b) the presence of carbon nanotubes (CNT) with closed and open tip, without containing the catalytic nanoparticles, was observed (marked with circles). This fact added to the good film adhesion suggests that the nucleation centers remained stuck to the substrate indicating a CNT basal growth mechanism, in accordance with Dupuis [11].

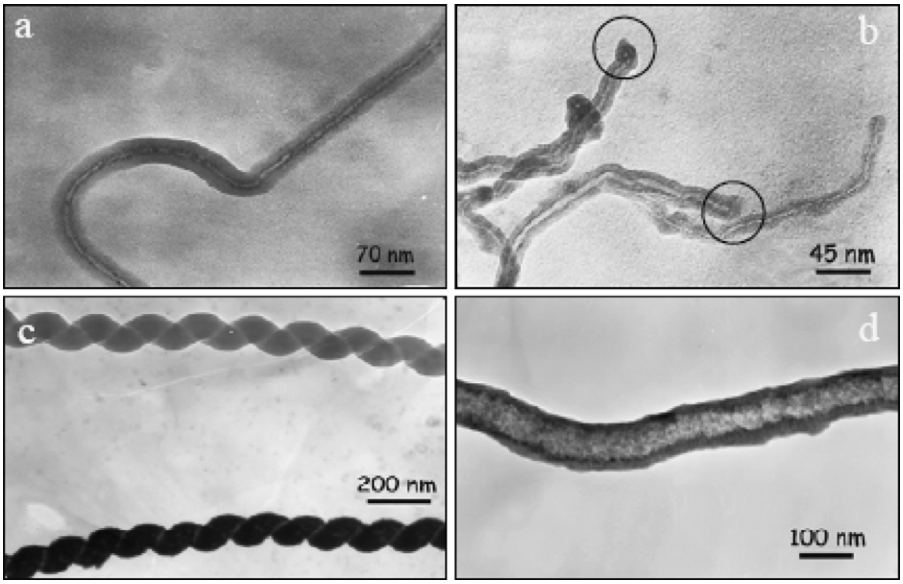

Fig. 4. TEM images of carbon nanostructures obtained: (a) floating potential, (b) ground potential, (c) and (d) −60 V.

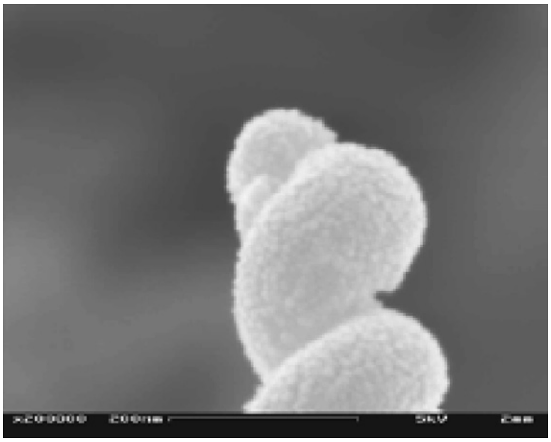

Fig. 5. FE-SEM image of surface of helical carbon nanofiber (HCNF).

4. Conclusion

Carbon nanostructures were synthesized by CVD using a Ni-film as precursor, deposited onto Si substrates applying a pulsed vacuum arc discharge. It was shown that the Ni-film morphology can be controlled changing the bias voltage applied during the deposition process. Besides, a correlation was found between the Ni film morphology and the characteristics of the CNS grown. At the highest roughness of the Ni film, mostly helical carbon nanofibers were synthesized, while carbon nanotubes were the predominant carbon nanostructure grown at low roughness. Moreover, on the smoothest Ni film, the carbon nanotubes with the lowest external diameter were synthesized. TEM image showed that the CNT were grown through the basal growth mechanism, which can be a consequence of the good adhesion between Ni-films and Si substrate obtained with the vacuum arc technique.

Acknowledgments

We thank the following institutions for their financial support: Universidad de Buenos Aires; Consejo Nacional de Investigaciones Científicas y Técnicas–Argentina and Agencia Nacional de Promoción Científica y Tecnológica - Argentina.

References

[1] P. Guo, T. Chen, Y. Chen, Z. Zhang, T. Feng, L. Wang, L. Lin, Z. Sun, Z.H. Zheng, Solid-State Electron. 52 (2008) 877–881.
[2] M. Escobar, M. Moreno, R. Candal, M. Marchi, A. Caso, P. Polosecki, G. Rubiolo, S. Goyanes, Appl. Surf. Sci. 254 (2007) 251–256.
[3] D. Zilli, C. Chiliotte, M. Escobar, V. Bekeris, G. Rubiolo, A. Cukierman, S. Goyanes, Polymer 46 (2005) 6090–6095.
[4] D. Zilli, S. Goyanes, M. Escobar, C. Chiliotte, V. Bekeris, A. Cukierman, G. Rubiolo, Polymer Comp. 28 (2007) 612–617.
[5] L. Zhang, Y. Tan, D. Resasco, Chem. Phys. Lett. 422 (2006) 198–203.
[6] S. Su, W. Chiang, C. Lin, M. Yokoyama, Phys. E: Low-Dimensional Syst. Nanostruct. 40 (2008) 2322–2326.
[7] P. Paredez, M. Maia da Costa, L. Zagonel, C. Ribeiro, F. Alvarez, Carbon 45 (2007) 2678–2684.
[8] L. Giuliani, D. Grondona, H. Kelly, F.O. Minotti, J. Phys. D: Appl. Phys. 40 (2007) 401–408.
[9] Y. Qin, L. Yu, Y. Wang, G. Li, Z. Cui, Solid State Commun. 138 (2006) 5–8.
[10] C. Chuang, W. Liu, W. Chen, J. Huang, Appl. Surf. Sci. 254 (2008) 4681–4687.
[11] A. Dupuis, Prog. Mater. Sci. 50 (2005) 929–961.